Published in final edited form as:
Vet Comp Oncol. 2008 March ; 6(1): 39–54. doi:10.1111/j.1476-5829.2007.00139.x.

NOD/SCID mouse model of canine T-cell lymphoma with humoral hypercalcaemia of malignancy: cytokine gene expression profiling and *in vivo* bioluminescent imaging

M. V. P. Nadella[1], **W. C. Kisseberth**[2], **K. S. Nadella**[3], **N. K. Thudi**[1], **D. H. Thamm**[4], **E. A. McNiel**[5], **A. Yilmaz**[1], **K. Boris-Lawrie**[1], and **T. J. Rosol**[1]

[1]Department of Veterinary Biosciences, The Ohio State University, Columbus, OH, USA

[2]Department of Veterinary Clinical Sciences, The Ohio State University, Columbus, OH, USA

[3]Human Cancer Genetics, The Ohio State University, Columbus, OH, USA

[4]Department of Clinical Sciences, College of Veterinary Medicine and Biomedical Sciences, Colorado State University, Fort Collins, CO, USA

[5]Department of Veterinary Clinical Sciences, University of Minnesota, St. Paul, MN, USA

Abstract

Lymphoma is a malignant neoplasm arising from B or T lymphocytes. In dogs, one-third of lymphomas are highly aggressive multicentric T-cell lymphomas that are often associated with humoral hypercalcaemia of malignancy (HHM). There are no cell lines or animal models to investigate the pathogenesis of T-cell lymphoma and HHM in dogs. We developed the first xenograft model by injecting lymphoma cells from an Irish Wolfhound intraperitoneally into NOD/SCID mice. The mice developed multicentric lymphoma along with HHM and increased parathyroid hormone-related protein (PTHrP) as occurs in dogs with T-cell lymphoma. Using cytokine complementary DNA arrays, we identified genes that have potential implications in the pathogenesis of T-cell lymphoma. Quantitative reverse transcriptase-polymerase chain reaction (RT-PCR) of T-cell lymphoma samples from hypercalcaemic canine patients showed that PTHrP likely plays a central role in the pathogenesis of HHM and that hypercalcaemia is the result of a combinatorial effect of different hypercalcaemic factors. Finally, we monitored *in vivo* tumour progression and metastases in the mouse model by transducing the lymphoma cells with a lentiviral vector that encodes a luciferase-yellow fluorescent protein reporter and showed that *in vivo* trafficking patterns in this model were similar to those seen in dogs. This unique mouse model will be useful for translational research in lymphoma and for investigating the pathogenesis of T-cell lymphoma and HHM in the dog.

Keywords

bioluminescent imaging; canine lymphoma; humoral hypercalcaemia of malignancy; PTHrP; xenograft

Correspondence address: Dr Thomas J. Rosol, Department of Veterinary, Biosciences, College of Veterinary Medicine, The Ohio State University, 1925 Coffey Road, Columbus, OH 43212, USA rosol.1@osu.edu.

Introduction

Non-Hodgkin ' s lymphoma (NHL) includes several malignant lymphoproliferative diseases that originate from lymphocytes and represents the fifth most common cause of cancer-related deaths in humans in the USA. [1] Lymphoma is the third most common neoplasm in dogs, 2 with an estimated annual incidence of approximately 33 per 10 0000 dogs. 3 In the absence of chemotherapy, survival beyond 1 month after diagnosis of lymphoma is uncommon. 4 The most common anatomic presentation of canine lymphoma is the multicentric form, which usually presents as superficial lymphadenopathy 5 with or without hepatosplenomegaly. About 26 – 38% of the lymphomas in dogs 6،7 and 15% of the lymphomas in humans [8] are T cell in origin. Humoral hypercalcaemia of malignancy (HHM) is a frequent paraneoplastic syndrome seen in approximately 40% of the dogs with T-cell lymphoma [9] and in 15% of humans with NHL. 10 In addition, 70% of human patients with adult T-cell leukaemia/lymphoma caused by human T-cell lymphotropic virus type-1 11 develop HHM. HHM is a multifactorial syndrome caused by the action of multiple factors produced by neoplastic cells affecting bone, kidney and intestine that disrupt normal calcium homeostasis. 12،13 The primary mechanism for hypercalcaemia in patients with lymphoma is increased osteoclastic bone resorption induced by humoral mediators. 14،[15] Factors produced by lymphoma implicated in the pathogenesis of HHM include parathyroid hormonerelated protein (PTHrP), calcitriol, transforming growth factors (TGFs), tumour necrosis factors (TNF), interleukin-1 (IL-1), interleukin-6 (IL-6), macrophage inflammatory protein-1 alpha (MIP-1α) and granulocyte colony-stimulating factor. [16 – 21] Calcitriol, the active product of vitamin D metabolism, enhances gastrointestinal calcium absorption and also mobilizes calcium from bone. Increased calcitriol production was reported in human NHL patients with hypercalcaemia and was implicated as a major humoral mediator in the pathogenesis of HHM in lymphoma; however, dysregulated calcitriol production was also observed in normocalcaemic patients with NHL. 10،19 Firkin *et al.* reported that NHL patients with hypercalcaemia had elevated circulating levels of PTHrP, with no increase in the levels of calcitriol. [22]

PTHrP originally was isolated from specific tumours as the primary cause of HHM 23 and is over-expressed by many different types of neoplasms. 24 Studies over the past several years have shown that PTHrP plays a primary role in HHM 25 and hypercalcaemia in tumour-bearing animals could be corrected using a neutralizing antibody to PTHrP. [26] Amino-terminal peptides of PTHrP have been shown to exert PTH-like actions in bone and kidney by binding to a common receptor for PTH/PTHrP (PTH-1 receptor), resulting in hypercalcaemia. [27،28] Our laboratory previously reported that dogs with lymphoma and hypercalcaemia have elevated levels of plasma PTHrP but that these levels were lower than in dogs with carcinomas and hypercalcaemia. Moreover, there was no significant correlation between serum calcium and PTHrP concentrations in dogs with lymphoma and hypercalcaemia, suggesting a role for other cytokines in this syndrome. 29 Factors such as TGFα, IL-1, IL-6 and TNF have been shown to enhance the hypercalcaemic effects of PTHrP. 30 Furthermore, TGFβ, TNFα and IL-1 have been reported to upregulate PTHrP gene expression in a variety of nonlymphoid cell lines and tissues. [31,32] We hypothesized that PTHrP plays a central role in the pathogenesis of HHM in dogs with T-cell lymphoma and acts synergistically with other cytokines produced by the tumour cells.

Canine lymphoma is a spontaneous disease that has a clinical presentation and biologic behaviour that closely resembles the human disease. [33] Furthermore, canine lymphoma is a useful translational model to study the pathogenesis and treatment of lymphoma because dogs share extensive genome homology and a common environment with humans. [34,35] The value of the canine model also depends on the availability of rodent models that can reproduce the disease as it occurs in dogs. Development of animal models that recapitulate the natural history of cancers and their clinical response to therapy is an important prerequisite for rapid bench-

to-bedside translation of anticancer therapies. [36] Moreover, the pathogenesis of HHM in dogs with T-cell lymphoma has not been investigated because of the lack of relevant *in vivo* models and little is known about PTHrP expression and its interrelationship with other cytokines. In this study, we report the development and characterization of a NOD/SCID mouse model of canine T-cell lymphoma with HHM that closely resembles the disease as it occurs in dogs and humans.

The study of animal models has been limited by the difficulty of accurately assessing disease burden and response to therapy. Measurement of tumour volume using callipers is limited to tumours that occur at accessible sites. [37] Some of the available *in vivo* models of haematological malignancies do not readily allow for sensitive, real-time detection of tumours or for serial measurements of tumour progression. [36] For this purpose, we developed canine lymphoma cells that stably express luciferase and yellow fluorescent protein (YFP), which allows imaging of tumour growth and metastasis *in vivo* in real time. Bioluminescent imaging (BLI), a noninvasive imaging technique, can be used to monitor the growth of luciferase-expressing lymphoma cells.

In this study, we demonstrated that NOD/SCID mice injected intraperitoneally with canine lymphoma cells develop multicentric lymphoma and HHM as observed in canine patients. The bioluminescent mouse model recapitulates the multicentric anatomical distribution of lymphoma, confirmed by histopathological analyses, and is consistent with the distribution of tumours in dogs and humans with lymphoma. Cytokine gene expression profiling revealed several genes that may contribute to tumourigenesis and metastasis in lymphoma. Furthermore, analysis of expression of potential hypercalcaemic factors in xenograft tumours and tumours from dogs with T-cell lymphoma and HHM using quantitative real-time RT-PCR showed that distinct hypercalcaemic factors were produced by these cells. Therefore, this study not only provides a clinically relevant *in vivo* model for more accurate preclinical evaluation of investigational therapies against lymphoma but also will permit mechanistic studies on the interrelationships between cytokines and PTHrP in the pathogenesis of HHM.

Materials and methods

Animals and lymphoma cell inoculations

Immunodeficient SCID/NOD (NOD CB17-PRKDCSCID/J) mice (Jackson Lab, Bar Harbor, ME, USA) were maintained under specific pathogen-free conditions in the animal facility of the College of Veterinary Medicine at The Ohio State University, Columbus, OH, USA. Lymphoma cells were obtained from a 4-year-old, intact, female Irish Wolfhound that was presented to the Veterinary Teaching Hospital, University of Wisconsin – Madison, Madison, WI, USA, with generalized lymphadenopathy, hepatosplenomegaly and hypercalcaemia (total calcium – 15.4 mg dL^{-1}). The lymphoma was CD3 positive and CD79a negative as determined by routine immunohistochemistry, and T-cell lymphoma was diagnosed. One of the popliteal lymph nodes from the dog was surgically excised, and the cells were passed through a #100 mesh stainless steel tissue sieve (Bellco, Vineland, NJ, USA) after dissecting away the capsule. The cells were washed three times with cold Hanks ' balanced salt solution/5 μM ethylenediaminetetraacetic acid (EDTA) and clumps were removed with a 40- μm nylon filter. The red blood cells were lysed with ACK lysing buffer (BioWhittaker, Walkersville, MD, USA) for 5 min at room temperature, followed by brief vortexing. The cells were kept frozen (90% foetal bovine serum and 10% dimethyl sulphoxide) in liquid nitrogen until use. Male mice (5 weeks old) were used as recipients and were injected intraperitoneally with 1.5×10^7 cells suspended in RPMI-1640 medium. Controls were inoculated with medium alone. The xenografted mice were sacrificed, and the tumours from the spleen and mesenteric lymph nodes were removed, minced, washed three times with RPMI-1640 medium containing 10% foetal

bovine serum, resuspended in RPMI-1640 medium and serially passaged into SCID/NOD mice approximately every 6–8 weeks.

Patient samples and normal canine lymph nodes

T-cell lymphomas (confirmed by immunohistochemistry, $CD3^{(+)}$ /$CD79a^{(-)}$) were collected from patients presented to the Veterinary Teaching Hospital at The Ohio State University, Columbus, OH, USA. A serum calcium concentration of greater than or equal to the laboratory reference value of 11.6 mg dL^{-1} was considered hypercalcaemic. The samples are represented as dog numbers with the total calcium (mg dL^{-1}) indicated in parenthesis: 1 (20.5), 2 (14.9), 3 (11.6), 4 (14.2), 5 (11.9) and 6 (17.9). Two popliteal lymph nodes were collected at necropsy from three control (healthy) experimental female Beagle dogs each and used as controls.

Histopathology, immunohistochemistry and immunofluorescence

Complete necropsies were performed on all mice. Tissues were fixed in 10% neutral-buffered formalin, embedded in paraffin, cut into 5-μm sections and stained with haematoxylin and eosin. Immunohistochemistry was performed on paraffin sections with the following antibodies: rabbit anti-human CD3 (1:100; DAKO, Carpinteria, CA, USA) and biotinylated goat anti-rabbit antibody (1:200; DAKO); mouse anti-human CD79 α cy (1:25; DAKO) and biotinylated horse anti-mouse antibody (1:200; DAKO). Visualization was achieved using diaminobenzidine (DAKO) and haematoxylin counterstain. Immunofluorescence staining was performed on a cytospin preparation of cells from ascites fluid. Briefly, the cells were fixed for 10 min in phosphate-buffered saline (PBS) containing 4% paraformaldehyde. The fixed cells were permeabilized with 0.1% Triton X-100 in PBS for 10 min and blocked with 5% bovine serum albumin in PBS for 1 h at room temperature. The cells were stained for 1 h at room temperature with polyclonal rabbit anti-PTHrP (PTHrP amino acids 34 – 53) (1:200, Ab-2; Oncogene Research Products, Cambridge, MA, USA), followed by incubation for 1 h with goat anti-rabbit IgG conjugated with fluorescein isothiocyanate (1:1000; Molecular Probes, Eugene, OR, USA). Confocal microscopy was performed using a Leica TCS SP2 AOBS Confocal Laser Scanning Microscope (Leica, Heidelberg, Germany).

Bone histomorphometry

Proximal tibiae were collected and fixed in 10% neutral-buffered formalin for 24 h at 4 °C, decalcified in 10% EDTA (pH 7.4) at 4 °C, dehydrated in graded series of ethanol for 5 days at 4 °C, infiltrated in two changes of glycol methacrylate (Poly-sciences, Warrington, PA, USA) for 10 days at 4 °C and embedded in glycol methacrylate at 4 °C. Sections were cut at 5 μm, histochemically stained for tartrate-resistant acid phosphatase (Sigma, St. Louis, MO, USA) and counterstained with haematoxylin. Measurements were performed using Image-Pro Plus version 5.0 (Media Cybernetics, Silver Spring, MD, USA) image analysis software. Histomorphometry was performed on 12 mice xenografted with canine T-cell lymphoma and compared with six age-matched control mice. Osteoclastic bone resorption was measured in trabecular bone, and osteoclasts were identified as cells lining trabecular bone that stained positive (red) for tartrate-resistant acid phosphatase. Measurements included total bone area, trabecular bone area and perimeter, osteoclast number per millimetre of trabecular bone and per cent osteoclast perimeter.

Polymerase chain reaction amplification of canine microsatellites

Genomic DNA was isolated using DNeasy Tissue Kit (Qiagen, Valencia, CA, USA) from control mouse spleen, whole blood from a dog (canine WB), Ace-1 cells (canine prostate cancer cell line) and mesenteric lymph nodes from the xenografted mice. DNA (100 ng) was amplified using primers specific for canine microsatellites FH2365, FH2356 34‚38 and C36672 as

described 39 using PCR Master Mix (Promega, Madison, WI, USA). The products were separated by electrophoresis on a 1.5% agarose gel for visualization.

Measurement of plasma calcium and PTHrP concentrations

Calcium and PTHrP plasma concentrations were measured in control and lymphoma-bearing mice. Blood was obtained from the femoral artery at necropsy. Total calcium concentrations were measured in 10 μL of heparinized plasma with a Vitros DT-60 II clinical chemistry analyser (Johnson & Johnson, Cornelia, GA, USA). Plasma PTHrP concentrations were measured using a two-site immunoradiometric assay (DSL, Webster, TX, USA) specific for the PTHrP N-terminal region (amino acids 1 – 40) and mid-region (amino acids 57 – 80).

Cytokine gene expression profiling

Panorama Human Cytokine Gene Arrays (Sigma-Genosys, St. Louis, MO, USA) were used to identify the cytokines involved in the pathogenesis of T-cell lymphoma. Total RNA was isolated using TRIZOL (Invitrogen, Carlsbad, CA, USA). Briefly, ^{32} P-radiolabeled complementary DNA (cDNA) probes were prepared from 2.5 μg of pooled total RNA using oligo dT and avian myelobastosis virus (AMV) reverse transcriptase at 42 °C and were purified on a Sephadex G-25 spin column (Sigma-Genosys). The arrays were hybridized overnight at 60 °C, washed and subjected to autoradiography for 12–72 h. The intensity of hybridization signals was quantified using ArrayVision software version 6.0 (Imaging Research, Haverhill, UK). The intensity of each spot was corrected for background levels and was normalized for differences in labelling using the average values of the housekeeping genes (β 2-microglubulin, β-actin, GAPDH, cyclophilin A, HPRT, HLA-A0201, L19, transferrin R and α-tubulin). For each gene, the normalized array data were compared as the ratio between lymphoma versus normal canine lymph node (NCLN). Genes that were upregulated or downregulated at least 2.5-fold or more were considered dysregulated.

Quantitative real-time RT-PCR

Total RNA was isolated from mouse lymph nodes with canine lymphoma, primary dog lymphomas and NCLN using TRIZOL (Invitrogen). Total RNA (5 μg) was reverse transcribed using the Superscript II First Strand cDNA synthesis kit (Invitrogen) and the final cDNA was diluted to 200 μL with RNase- and DNase-free water. Quantitative RT-PCR (qRT-PCR) was performed with 5 μL of the cDNA in a 25-μL volume in triplicate using ABI PRISM 7900HT Sequence Detection System (Applied Biosystems, Foster City, CA, USA) with a standard temperature protocol and 2× SYBR Green PCR Master Mix reagent (Applied Biosystems). As a control, the messenger RNA (mRNA) level of glyceraldehyde-3 phosphate dehydrogenase (GAPDH) was determined in the real-time polymerase chain reaction (PCR) assay for each RNA sample and used to normalize the data. Fold changes were calculated by the $2^{-\Delta\Delta CT}$ method as described by the manufacturer (Applied Biosystems). Canine-specific primers for IL-6, TNF α, TGFβ, GAPDH 40،41 and IL-1α 42 were used as described. Primers for IL-1β, TGFα, TNFβ, PTHrP, receptor activator for nuclear factor κB ligand (RANKL) and MIP-1α were designed by aligning the human sequence with the dog genome at http://genome.ucsc.edu/cgi-bin/hgBlat and are shown in Table 1.

Generation of lentiviral vectors and transduction of lymphoma cells

Retroviral transduction was performed using vectors encoding luciferase-YFP, generated as described previously. [43] The xenografted lymph nodes were minced into 0.25 – 0.5 mm^3 pieces and transduced with 7.2×10^6 infectious viral particles by spin inoculation at 1467 *g* for 1 h at 32 °C. Polybrene was added at a final concentration of 8 μg mL^{-1}. Following transduction, the tissues were incubated in a cell culture incubator at 37 °C for 1 h and washed twice with RPMI-1640 medium before injection into mice.

In vivo and *ex vivo* imaging

Mice were injected intraperitoneally with 150 μL (40 mg mL^{-1}) luciferin (Xenogen, Alameda, CA, USA) dissolved in PBS. Anaesthesia was induced using a 3% isoflurane – air mixture and maintained at 1.5% isoflurane. Mice were placed in the light-impermeable imaging chamber of the IVIS imaging system (Xenogen), and the photons emitted from luciferase-expressing cells were quantified and analysed using LivingImage software version 2.50 (Xenogen). For *ex vivo* imaging, luciferin was injected into the mice immediately prior to necropsy, and tissues were collected after humane euthanasia and imaged.

Statistical analysis

Student ' s *t*-test was performed to compare the plasma calcium, PTHrP and bone histomorphometric parameters between the control mice and the mice bearing canine lymphoma xenografts. *t*-tests were used to compare the cytokine mRNA expression profiles between NCLN and xenograft lymphomas from the mice. A *P* value less than 0.05 was considered statistically significant.

Results

Xenografted dog lymphoma grew in NOD/SCID mice

Canine lymphoma cells inoculated intraperitoneally into SCID/NOD mice successfully engrafted and produced tumours (Fig. 1). The mice (83%, 13 of 16) had diffuse lymphoma in the mesenteric lymph nodes. Moderate to marked splenomegaly was present in 66% (10 of 16) of the mice (Fig. 1B). Small, white raised tumours were present in the liver in 66% of the mice (10 of 16). Tumours also were present in the mandibular lymph nodes in three mice (Fig. 1C). Moderate amounts of ascites were present in four of 16 mice. The thymus was approximately six to eight times larger than controls in two of the 16 mice (Fig. 1D). Microscopic evaluation of the mice (Table 2) inoculated with canine lymphoma cells revealed lymphoma in the mesenteric lymph nodes (14 of 16 mice) (Fig. 1J), spleen (14 of 16 mice), liver (12 of 16 mice) (Fig. 1I), kidney (10 of 16 mice), lung (eight of 16 mice) (Fig. 1K) and the thymus (two of 16 mice). In the mesentery and the spleen, solid sheets of large round cells replaced most of the normal tissue. The cells had a large round to oval nucleus, with a moderate amount of cytoplasm and a high mitotic index (4 per high power field, 400×).

Lymphomas were T-cell and of canine origin

The mesenteric lymph nodes from the xenografted mice demonstrated positive immunoreactivity for CD3 but not for CD79αcy, confirming the T-cell origin of the lymphomas (Fig. 1E,F). Because specific antibodies to detect canine antigens (that do not cross-react with the mouse) were not available, we used a novel PCR-based technique to amplify canine microsatellites. A specific PCR product was amplified for canine microsatellites FH2365, FH2356 (data not presented) and C36672 from the genomic DNA of the lymphoma xenografts, normal canine tissue and canine prostate cancer cell line (Ace-1) but not from the control mouse spleen (Fig. 1G), confirming canine origin of the lymphoma.

Plasma calcium concentration

Lymphoma-bearing mice had a statistically significant ($P < 0.005$) increase in total calcium (10.9 ± 0.8 mg dL^{-1}) concentrations compared with control mice (9.2 ± 0.1 mg dL^{-1}) (Fig. 2). Total calcium concentrations were as high as 12.4 mg dL^{-1} in mice with lymphoma.

Hypercalcaemic factors in lymphoma-bearing mice

Plasma PTHrP concentrations were increased in mice with lymphoma (3.2 ± 2.0 pM L^{-1}) compared with the control mice (<1.5 pM L^{-1}; Fig. 3A). PTHrP was present predominantly

and diffusely in the cytoplasm of neoplastic xenograft cells with some nuclear staining as evaluated by immunofluorescence microscopy (Fig. 1L). The xenografted canine lymphomas expressed PTHrP mRNA at significantly higher level (30-fold) than NCLN. In addition to PTHrP, the xenografted cells also expressed moderately increased levels of TNFα mRNA (three- to five-fold). There was mild (but not statistically significant) upregulation of TGFβ (two-fold) and RANKL (three-fold) mRNA in the xenografted canine lymphoma cells compared with NCLNs (Fig. 3B). There was a significant down-regulation of IL-6 mRNA (data not shown) in the xenografted lymphoma cells compared with the NCLNs. Although not statistically significant, the xenografted cells had a trend towards downregulation of IL-1β, TNFβ and TGFβ mRNA compared with NCLN.

Bone histomorphometry

To examine parameters of osteoclastic bone resorption, bone histomorphometric analysis was performed. There was no significant difference in the trabecular bone volume in the xenografted mice with lymphoma when compared with controls (Fig. 4A). The perimeter of trabecular bone lined by osteoclasts and the number of osteoclasts per millimetre of trabecular bone were increased approximately two-fold (Fig. 4B,C respectively) in NOD/SCID mice xenografted with canine T-cell lymphoma compared with controls ($P < 0.05$).

Microarray analysis of cytokines

To allow rapid screening of cytokines potentially involved in the pathogenesis of lymphoma, we compared cytokine gene expression profiles between lymphoma xenografts and NCLNs using the Panorama Human Cytokine Array. Of 865 different cytokines and chemokines present, 34 genes were significantly upregulated and 18 genes downregulated in the xenografts compared with the NCLNs. The list of genes dysregulated in xenografts compared with the normal lymph nodes is shown in Table 3. The upregulated genes included those involved in signal transduction, cell surface proteins, integrins and G-protein-coupled receptors. The downregulated genes included fibroblast growth factor (FGF) receptor-1, binding proteins and interleukin receptors. Quantitative real-time RT-PCR for integrin α4, integrin β9 (data not presented) and IL-1 receptor-like 2 (IL-1RL2) genes validated the microarray findings (Fig. 5).

Canine T-cell lymphomas express distinct hypercalcaemic factors

To identify the osteoclastogenic factors involved in the pathogenesis of HHM in dogs with T-cell lymphoma, we compared the mRNA levels of various hypercalcaemic cytokines using quantitative real-time RT-PCR in canine T-cell lymphoma samples from six hypercalcaemic dogs (Fig. 6). The samples from hypercalcaemic T-cell lymphoma dogs expressed very high levels of PTHrP mRNA compared to lymph nodes from normal dogs (69 ± 71-fold). The expression of PTHrP mRNA levels from lymphoma samples ranged from 2- to 194-fold higher than normal lymph nodes. While the expression of TNFα mRNA was upregulated in two dogs with lymphomas compared to NCLN, there was decreased TNFα expression in two lymphoma and no TNFα expression in two lymphoma samples (dogs 6 and 8) compared with NCLN. There was a mild upregulation of IL-1β mRNA (1.6- to 25-fold) in the lymphoma samples compared with NCLN. There was a mild upregulation of RANKL mRNA (2.3 ± 1.2-fold) in the lymphoma samples compared with NCLN. There was moderate downregulation of IL-6 mRNA and PTHrP (pM) IL-1α mRNA in the lymphoma samples compared to NCLN. There was no difference in the expression of TNFβ, TGFα and MIP-1α mRNA between the lymphoma samples and NCLN as shown in Fig. 6.

Tumours were detected by *in vivo* and *ex vivo* imaging

Because the canine lymphoma cells could not be maintained in culture, a retroviral transduction system was used for the delivery of a luciferase-YFP fusion gene. The time course of engraftment of canine lymphoma cells after intraperitoneal injection into SCID/NOD mice is shown in Fig. 7A. The recipients had detectable tumour growth 1 week after the injection of lymphoma cells. Repetitive imaging of mice at weekly intervals demonstrated lymphoma growth in the abdominal viscera. Tumour engraftment and progressive tumour growth was readily demonstrable by BLI several weeks before the animals appeared sick as monitored by dehydration and depression. At 7–8 weeks, BLI revealed widespread lymphoma growth in the mesenteric lymph nodes, with metastasis to the spleen, liver and lungs, which was confirmed by *ex vivo* imaging of these organs as shown in Fig. 7B.

Discussion

Lymphoma is a common malignancy in humans and dogs. Animal models that can be easily evaluated are critically important to enhance our understanding of the pathogenesis of lymphoma and for the development of more effective therapies. There are few animal models that closely recapitulate the disease as it occurs in both species, and there are no animal models that are useful for investigating the molecular pathogenesis of lymphoma and hypercalcaemia in dogs. We report the establishment of a model of canine T-cell lymphoma and HHM in NOD/SCID mice with lymphoma cells from a dog with HHM. The primary lymphoma cells produced multicentric lymphoma in NOD/SCID mice and maintained their morphological, immunohistochemical and molecular features. The xenografted lymphoma cells in NOD/SCID mice induced hypercalcaemia by upregulation of PTHrP and TNFα that stimulate osteoclastic bone resorption. Histomorphometric analysis showed that the HHM in mice bearing canine lymphoma was due to increased osteoclastic bone resorption as seen in human and canine patients with lymphoma and HHM.

There is little information on the pathogenesis of HHM in humans with lymphoma because of the lack of *in vivo* models. To our knowledge, the only available mouse models of lymphoma with HHM are for adult T-cell leukaemia/lymphoma (ATLL) in which hypercalcaemia occurs with a very high frequency. We established a SCID/beige mouse model of ATLL with HHM and have shown that hypercalcaemia in those mice was mediated primarily by increased levels of PTHrP. [44] Similarly, increased PTHrP is associated with HHM in this canine T-cell lymphoma xenograft mouse model and will be very useful for investigating the pathogenesis of HHM in lymphoma.

DNA microarrays represent a powerful tool for rapid screening of expression of many genes in parallel and have been used extensively for the study of gene expression in a variety of lymphoid malignancies. [45] To identify the molecular basis underlying the pathogenesis of T-cell lymphoma, we used a cDNA microarray to characterize the cytokine gene expression profiles of the canine lymphoma xenograft. Human cDNA arrays could be used to study comparative cytokine gene expression in canine lymphoma because of the extensive genetic homology between the two species. Using this technique, we identified a variety of genes that have potential implications in the tumourigenesis and metastases of canine lymphoma. For example, the upregulation of cell cycle regulator *cdk4* has been reported in a variety of solid tumours such as breast carcinoma, [46] mantle cell lymphoma [47] and diffuse large B-cell lymphoma. 48 Histone deacetylase has been shown to be upregulated in several solid tumours such as prostate, 49 breast 50 and gastric cancer. 51 Upregulation of matrix metalloproteinase-9 (MMP-9) has been reported to be a key player in the dissemination of T-cell lymphoma cells to peripheral tissues. 52 Integrins have been a subject of extensive research, and several antagonists of integrins are currently being evaluated as anticancer therapeutics. Integrins have been shown to promote cellular migration and survival in tumours and primary cells 53 and

have been shown to be involved in specific homing of lymphocytes to various tissues. 54 For example, it has been shown that integrin α4β7 targets T cells to the gut-associated lymphoid tissue (GALT). 55 Interestingly, upregulation of integrin α4 and β7 might explain the predominance of mesenteric lymphomas seen in our model. Genes such as the IL-1RL2 have been shown to be downregulated several fold in mantle cell lymphoma, 56 consistent with our observations; however, instead of TNF receptor superfamily-1A (TNFRSF1A), rather TNFRSF1B was downregulated in our lymphoma model.

Many dogs with T-cell lymphoma develop HHM, a paraneoplastic syndrome that significantly contributes to morbidity and mortality when it occurs. [57] PTHrP has been shown to be a causative factor of hypercalcaemia in several epithelial cancers in humans and in animals bearing human solid tumours. [26,58] A previous investigation by our laboratory showed that dogs with lymphoma and hypercalcaemia had increased concentrations of plasma PTHrP, but there was no correlation between serum calcium and PTHrP levels. [29] It was suggested that PTHrP induced HHM in synergy with tumour-related cytokines. Kubota *et al.* reported increased plasma PTHrP in one dog with lymphoma and hypercalcaemia, and no detectable PTHrP in dogs with lymphoma and normocalcaemia and in healthy dogs. They also detected PTHrP mRNA expression in one dog with lymphoma and hypercalcaemia and four dogs with lymphoma and normocalcaemia. [59] In this study, we examined the expression profiles of various cytokines capable of mediating bone resorption in dogs with T-cell lymphoma and hypercalcaemia. Comparison of the mRNA levels in six hypercalcaemic dogs with T-cell lymphoma revealed a distinct set of hypercalcaemic factors in each case. PTHrP mRNA was upregulated in all hypercalcaemic dogs and ranged from 3- to 194-fold. TNFα mRNA was either moderately upregulated or downregulated in hypercalcaemic dogs. TNFα, a proinflammatory cytokine, is known to stimulate osteoclastogenesis by RANKL-dependent60 and RANKL-independent mechanisms.61 Also, TNFα has been shown to be involved in the pathogenesis of several inflammatory and metabolic bone diseases such as rheumatoid arthritis, periodontitis and/or postmenopausal osteoporosis.62 The upregulation of TNFα mRNA in some of the lymphoma samples suggests a potential role for TNFα in the pathogenesis of HHM. RANKL, secreted by activated T lymphocytes, has been shown to promote differentiation and fusion of osteoclast precursors and activate mature osteoclasts by binding to its specific receptor, RANK. [63] There was a mild to moderate upregulation of RANKL in some of the hypercalcaemic lymphoma samples (dogs 2, 4 and 5), which likely contributed to the pathogenesis of HHM in those dogs. Although IL-6 has been shown to be upregulated in some cancers with HHM, we found downregulation of IL-6 in all the samples examined. For example in dog 1, there was mild to moderate upregulation of PTHrP with a moderate to marked upregulation of TNFα and IL-1β, suggesting a possible synergistic role of TNFα and IL-1β with PTHrP in causing HHM. In summary, as indicated by Cox *et al.*, because of the heterogeneity of the lymphomas[64] and particularly of T-cell lymphomas, a common cause of hypercalcaemia is unlikely. In spite of these differences, our study has revealed that PTHrP likely plays a central role in the pathogenesis of HHM in dogs with T-cell lymphoma and it is likely that hypercalcaemia in each case is the result of a combinatorial effect of different sets of cytokines, and in this context the roles of various cytokines must be evaluated.

The investigation of mechanisms of tumour growth and metastasis and response to therapy requires animal models capable of detecting small numbers of cells and assessing disease burden non-invasively and quantitatively. Because lentiviral vectors can infect nondividing cells and because our xenografted lymphoma cells do not grow *in vitro*, we used a novel lentiviral transduction technique. The lentiviral vectors were very useful and efficient for delivering the reporter transgene into tumour cells that do not grow *in vitro*. Using BLI, we were able to detect and monitor lymphoma cell growth in locations that were not easily monitored grossly such as the abdominal cavity and viscera. Tumour cell trafficking,

engraftment in different organs and metastasis could be visualized without perturbing intact organs. BLI showed that trafficking of lymphoma cells in this NOD/SCID mouse model has similarities to that in dogs and humans with lymphoma involving the lymph nodes, liver and spleen. The abdominal/mesenteric distribution of the tumour seen in this model is not a common clinical presentation in dogs. This could be either because of the intraperitoneal route of injection of tumour cells or because of specific host (species) factors that influence tumour cell trafficking and anatomic distribution of the tumours in dogs and mice.

In conclusion, this bioluminescent NOD/SCID mouse model of canine T-cell lymphoma provides a clinically relevant *in vivo* model to study the regulation of PTHrP and its interrelationships with cytokines produced by lymphoma cells in the induction of HHM. This new tool will improve our understanding of tumour biology and facilitate drug discovery and evaluation.

Acknowledgments

This study was supported by the Glenn C. Barber Fund from the College of Veterinary Medicine, The Ohio State University (M. V. P. N.), the National Cancer Institute (CA 100730) (T. J. R.) and by grant D00CA-25 from the Morris Animal Foundation (D. H. T.).

References

1. O'Connor OA, Toner LE, Vrhovac R, Budak-Alpdogan T, Smith EA, Bergman P. Comparative animal models for the study of lymphohematopoietic tumors: strengths and limitations of present approaches. Leukemia & Lymphoma 2005;46:973–992. [PubMed: 16019548]
2. Sueiro FA, Alessi AC, Vassallo J. Canine lymphomas: a morphological and immunohistochemical study of 55 cases, with observations on p53 immunoexpression. Journal of Comparative Pathology 2004;131:207–213. [PubMed: 15276860]
3. Teske E. Canine malignant lymphoma: a review and comparison with human non-Hodgkin's lymphoma. Veterinary Quarterly 1994;16:209–219. [PubMed: 7740746]
4. MacEwen EG. Spontaneous tumors in dogs and cats: models for the study of cancer biology and treatment. Cancer Metastasis Reviews 1990;9:125–136. [PubMed: 2253312]
5. Washizu T, Azakami D, Bonkobara M, Washizu M, Arai T. Changes in activities of enzymes related to energy metabolism in canine lymphoma cells. Journal of Veterinary Medical Science 2005;67:615–616. [PubMed: 15997191]
6. Modiano JF, Breen M, Burnett RC, Parker HG, Inusah S, Thomas R, Avery PR, Lindblad-Toh K, Ostrander EA, Cutter GC, Avery AC. Distinct B-cell and T-cell lymphoproliferative disease prevalence among dog breeds indicates heritable risk. Cancer Research 2005;65:5654–5661. [PubMed: 15994938]
7. Fournel-Fleury C, Magnol JP, Bricaire P, Marchal T, Chabanne L, Delverdier A, Bryon PA, Felman P. Cytohistological and immunological classification of canine malignant lymphomas: comparison with human non-Hodgkin's lymphomas. Journal of Comparative Pathology 1997;117:35–59. [PubMed: 9263843]
8. The Non-Hodgkin'ls Lymphoma Classification Project. A clinical evaluation of the International Lymphoma Study Group classification of non-Hodgkin's lymphoma. Blood 1997;89:3909–3918. [PubMed: 9166827]
9. Fournel-Fleury C, Ponce F, Felman P, Blavier A, Bonnefont C, Chabanne L, Marchal T, Cadore JL, Goy-Thollot I, Ledieu D, Ghernati I, Magnol JP. Canine T-cell lymphomas: a morphological, immunological, and clinical study of 46 new cases. Veterinary Pathology 2002;39:92–109. [PubMed: 12102223]
10. Seymour JF, Gagel RF, Hagemeister FB, Dimopoulos MA, Cabanillas F. Calcitriol production in hypercalcemic and normocalcemic patients with non-Hodgkin lymphoma. Annals of Internal Medicine 1994;121:633–640. [PubMed: 7944070]

11. Nosaka K, Miyamoto T, Sakai T, Mitsuya H, Suda T, Matsuoka M. Mechanism of hypercalcemia in adult T-cell leukemia: overexpression of receptor activator of nuclear factor kappaB ligand on adult T-cell leukemia cells. Blood 2002;99:634–640. [PubMed: 11781248]
12. Rosol TJ, Capen CC. Mechanisms of cancer-induced hypercalcemia. Laboratory Investigation 1992;67:680–702. [PubMed: 1460860]
13. Mundy GR, Guise TA. Hypercalcemia of malignancy. American Journal of Medicine 1997;103:134–145. [PubMed: 9274897]
14. Roodman GD. Mechanisms of bone lesions in multiple myeloma and lymphoma. Cancer 1997;80:1557–1563. [PubMed: 9362422]
15. Meuten DJ, Kociba GJ, Capen CC, Chew DJ, Segre GV, Levine L, Tashjian AH Jr, Voelkel EF, Nagode LA. Hypercalcemia in dogs with lymphosarcoma. Biochemical, ultrastructural, and histomorphometric investigations. Laboratory Investigation 1983;49:553–562. [PubMed: 6314038]
16. Yoneda T, Alsina MA, Chavez JB, Bonewald L, Nishimura R, Mundy GR. Evidence that tumor necrosis factor plays a pathogenetic role in the paraneoplastic syndromes of cachexia, hypercalcemia, and leukocytosis in a human tumor in nude mice. Journal of Clinical Investigation 1991;87:977–985. [PubMed: 1999505]
17. Mundy GR. Pathophysiology of cancer-associated hypercalcemia. Seminars in Oncology 1990;17:10–15. [PubMed: 2185548]
18. Johnson RA, Boyce BF, Mundy GR, Roodman GD. Tumors producing human tumor necrosis factor induced hypercalcemia and osteoclastic bone resorption in nude mice. Endocrinology 1989;124:1424–1427. [PubMed: 2917519]
19. Seymour JF, Gagel RF. Calcitriol: the major humoral mediator of hypercalcemia in Hodgkin's disease and non-Hodgkin's lymphomas. Blood 1993;82:1383–1394. [PubMed: 8364192]
20. Wano Y, Hattori T, Matsuoka M, Takatsuki K, Chua AO, Gubler U, Greene WC. Interleukin 1 gene expression in adult T cell leukemia. Journal of Clinical Investigation 1987;80:911–916. [PubMed: 2887587]
21. Niitsu Y, Urushizaki Y, Koshida Y, Terui K, Mahara K, Kohgo Y, Urushizaki I. Expression of TGF-beta gene in adult T cell leukemia. Blood 1988;71:263–266. [PubMed: 2891388]
22. Firkin F, Seymour JF, Watson AM, Grill V, Martin TJ. Parathyroid hormone-related protein in hypercalcaemia associated with haematological malignancy. British Journal of Haematology 1996;94:486–492. [PubMed: 8790147]
23. Rosol TJ, Capen CC. Pathogenesis of humoral hypercalcemia of malignancy. Domestic Animal Endocrinology 1988;5:1–21. [PubMed: 3066580]
24. Broadus AE, Mangin M, Ikeda K, Insogna KL, Weir EC, Burtis WJ, Stewart AF. Humoral hypercalcemia of cancer. Identification of a novel parathyroid hormone-like peptide. New England Journal of Medicine 1988;319:556–563. [PubMed: 3043221]
25. Wysolmerski JJ, Broadus AE. Hypercalcemia of malignancy: the central role of parathyroid hormone-related protein. Annual Review of Medicine 1994;45:189–200.
26. Kukreja SC, Shevrin DH, Wimbiscus SA, Ebeling PR, Danks JA, Rodda CP, Wood WI, Martin TJ. Antibodies to parathyroid hormone-related protein lower serum calcium in athymic mouse models of malignancy-associated hypercalcemia due to human tumors. Journal of Clinical Investigation 1988;82:1798–1802. [PubMed: 2846659]
27. Caulfield MP, McKee RL, Goldman ME, Thiede MA, Thompson DD, Fisher JE, Levy JJ, Seedor JG, Horiuchi N, Clemens TL. Parathyroid hormone-related protein (PTHrP): studies with synthetic peptides indicate that parathyroid hormone and PTHrP interact with the same receptor. International Journal of Radiation Applications and Instrumentation B 1990;17:633–637.
28. Rosenblatt M, Caulfield MP, Fisher JE, Horiuchi N, McKee RL, Rodan SB, Thiede MA, Thompson DD, Seedor JG, Nutt RE. A tumor-secreted protein associated with human hypercalcemia of malignancy. Biology and molecular biology. Annals of the New York Academy Sciences 1988;548:137–145.
29. Rosol TJ, Nagode LA, Couto CG, Hammer AS, Chew DJ, Peterson JL, Ayl RD, Steinmeyer CL, Capen CC. Parathyroid hormone (PTH)-related protein, PTH, and 1,25-dihydroxyvitamin D in dogs with cancer-associated hypercalcemia. Endocrinology 1992;131:1157–1164. [PubMed: 1505457]

30. Clines GA, Guise TA. Hypercalcaemia of malignancy and basic research on mechanisms responsible for osteolytic and osteoblastic metastasis to bone. Endocrine-Related Cancer 2005;12:549–583. [PubMed: 16172192]

31. Uy HL, Mundy GR, Boyce BF, Story BM, Dunstan CR, Yin JJ, Roodman GD, Guise TA. Tumor necrosis factor enhances parathyroid hormone-related protein-induced hypercalcemia and bone resorption without inhibiting bone formation *in vivo*. Cancer Research 1997;57:3194–3199. [PubMed: 9242449]

32. Boyce BF, Aufdemorte TB, Garrett IR, Yates AJ, Mundy GR. Effects of interleukin-1 on bone turnover in normal mice. Endocrinology 1989;125:1142–1150. [PubMed: 2788075]

33. Modiano JF, Breen M, Valli VE, Wojcieszyn JW, Cutter GR. Predictive value of p16 or Rb inactivation in a model of naturally occurring canine non-Hodgkin's lymphoma. Leukemia 2007;21:184–187. [PubMed: 16990767]

34. Starkey MP, Scase TJ, Mellersh CS, Murphy S. Dogs really are man's best friend – canine genomics has applications in veterinary and human medicine! Briefings in Functional Genomics & Proteomics 2005;4:112–128. [PubMed: 16102268]

35. Vail DM, MacEwen EG. Spontaneously occurring tumors of companion animals as models for human cancer. Cancer Investigation 2000;18:781–792. [PubMed: 11107448]

36. Mitsiades CS, Mitsiades NS, Bronson RT, Chauhan D, Munshi N, Treon SP, Maxwell CA, Pilarski L, Hideshima T, Hoffman RM, Anderson KC. Fluorescence imaging of multiple myeloma cells in a clinically relevant SCID/NOD *in vivo* model: biologic and clinical implications. Cancer Research 2003;63:6689–6696. [PubMed: 14583463]

37. Edinger M, Cao YA, Verneris MR, Bachmann MH, Contag CH, Negrin RS. Revealing lymphoma growth and the efficacy of immune cell therapies using *in vivo* bioluminescence imaging. Blood 2003;101:640–648. [PubMed: 12393519]

38. Mellersh CS, Langston AA, Acland GM, Fleming MA, Ray K, Wiegand NA, Francisco LV, Gibbs M, Aguirre GD, Ostrander EA. A linkage map of the canine genome. Genomics 1997;46:326–336. [PubMed: 9441735]

39. Ostrander EA, Mapa FA, Yee M, Rine J. One hundred and one new simple sequence repeat-based markers for the canine genome. Mammalian Genome 1995;6:192–195. [PubMed: 7749226]

40. Peeters D, Peters IR, Clercx C, Day MJ. Real-time RT-PCR quantification of mRNA encoding cytokines, CC chemokines and CCR3 in bronchial biopsies from dogs with eosinophilic bronchopneumopathy. Veterinary Immunology and Immunopathology 2006;110:65–77. [PubMed: 16226318]

41. Peeters D, Peters IR, Farnir F, Clercx C, Day MJ. Real-time RT-PCR quantification of mRNA encoding cytokines and chemokines in histologically normal canine nasal, bronchial and pulmonary tissue. Veterinary Immunology and Immunopathology 2005;104:195–204. [PubMed: 15734540]

42. Aihara Y, Kasuya H, Onda H, Hori T, Takeda J, Faraci FM. Quantitative analysis of gene expressions related to inflammation in canine spastic artery after subarachnoid hemorrhage [editorial comment]. Stroke 2001;32:212–217. [PubMed: 11136939]

43. Tannehill-Gregg SH, Levine AL, Nadella MV, Iguchi H, Rosol TJ. The effect of zoledronic acid and osteoprotegerin on growth of human lung cancer in the tibias of nude mice. Clinical and Experimental Metastasis 2006;23:19–31. [PubMed: 16715352]

44. Richard V, Lairmore MD, Green PL, Feuer G, Erbe RS, Albrecht B, D'Souza C, Keller ET, Dai J, Rosol TJ. Humoral hypercalcemia of malignancy: severe combined immunodeficient/beige mouse model of adult T-cell lymphoma independent of human T-cell lymphotropic virus type-1 tax expression. American Journal of Pathology 2001;158:2219–2228. [PubMed: 11395400]

45. Staudt LM. Gene expression profiling of lymphoid malignancies. Annual Review of Medicine 2002;53:303–318.

46. An HX, Beckmann MW, Reifenberger G, Bender HG, Niederacher D. Gene amplification and overexpression of CDK4 in sporadic breast carcinomas is associated with high tumor cell proliferation. American Journal of Pathology 1999;154:113–118. [PubMed: 9916925]

47. Hernandez L, Bea S, Pinyol M, Ott G, Katzenberger T, Rosenwald A, Bosch F, Lopez-Guillermo A, Delabie J, Colomer D, Montserrat E, Campo E. CDK4 and MDM2 gene alterations mainly occur in

highly proliferative and aggressive mantle cell lymphomas with wild-type INK4a/ARF locus. Cancer Research 2005;65:2199–2206. [PubMed: 15781632]

48. Rao PH, Houldsworth J, Dyomina K, Parsa NZ, Cigudosa JC, Louie DC, Popplewell L, Offit K, Jhanwar SC, Chaganti RSK. Chromosomal and gene amplification in diffuse large B-Cell lymphoma. Blood 1998;92:234–240. [PubMed: 9639522]
49. Patra SK, Patra A, Dahiya R. Histone deacetylase and DNA methyltransferase in human prostate cancer. Biochemical Biophysical Research Communications 2001;287:705–713.
50. Vigushin DM, Ali S, Pace PE, Mirsaidi N, Ito K, Adcock I, Coombes RC. Trichostatin A is a histone deacetylase inhibitor with potent antitumor activity against breast cancer *in vivo*. Clinical Cancer Research 2001;7:971–976. [PubMed: 11309348]
51. Choi JH, Kwon HJ, Yoon BI, Kim JH, Han SU, Joo HJ, Kim DY. Expression profile of histone deacetylase 1 in gastric cancer tissues. Japanese Journal of Cancer Research 2001;92:1300–1304. [PubMed: 11749695]
52. Aoudjit F, Potworowski EF, St Pierre Y. Bidirectional induction of matrix metalloproteinase-9 and tissue inhibitor of matrix metalloproteinase-1 during T lymphoma/endothelial cell contact: implication of ICAM-1. Journal of Immunology 1998;160:2967–2973.
53. Jin H, Varner J. Integrins: roles in cancer development and as treatment targets. British Journal of Cancer 2004;90:561–565. [PubMed: 14760364]
54. Drillenburg P, Pals ST. Cell adhesion receptors in lymphoma dissemination. Blood 2000;95:1900–1910. [PubMed: 10706853]
55. Schweighoffer T, Tanaka Y, Tidswell M, Erle DJ, Horgan KJ, Luce GE, Lazarovits AI, Buck D, Shaw S. Selective expression of integrin alpha 4 beta 7 on a subset of human CD4+ memory T cells with hallmarks of gut-trophism. Journal of Immunology 1993;151:717–729.
56. Hofmann WK, de Vos S, Tsukasaki K, Wachsman W, Pinkus GS, Said JW, Koeffler HP. Altered apoptosis pathways in mantle cell lymphoma detected by oligonucleotide microarray. Blood 2001;98:787–794. [PubMed: 11468180]
57. Gerber B, Hauser B, Reusch CE. Serum levels of 25-hydroxycholecalciferol and 1,25-dihydroxycholecalciferol in dogs with hypercalcaemia. Veterinary Research Communications 2004;28:669–680. [PubMed: 15609867]
58. Kukreja SC, Rosol TJ, Wimbiscus SA, Shevrin DH, Grill V, Barengolts EI, Martin TJ. Tumor resection and antibodies to parathyroid hormone-related protein cause similar changes on bone histomorphometry in hypercalcemia of cancer. Endocrinology 1990;127:305–310. [PubMed: 2361475]
59. Kubota A, Kano R, Mizuno T, Hisasue M, Moore PF, Watari T, Tsujimoto H, Hasegawa A. Parathyroid hormone-related protein (PTHrP) produced by dog lymphoma cells. Journal of Veterinary Medical Science 2002;64:835–837. [PubMed: 12399610]
60. Azuma Y, Kaji K, Katogi R, Takeshita S, Kudo A. Tumor necrosis factor-alpha induces differentiation of and bone resorption by osteoclasts. Journal of Biological Chemistry 2000;275:4858–4864. [PubMed: 10671521]
61. Kobayashi K, Takahashi N, Jimi E, Udagawa N, Takami M, Kotake S, Nakagawa N, Kinosaki M, Yamaguchi K, Shima N, Yasuda H, Morinaga T, Higashio K, Martin TJ, Suda T. Tumor necrosis factor alpha stimulates osteoclast differentiation by a mechanism independent of the ODF/RANKL-RANK interaction. Journal of Experimental Medicine 2000;191:275–286. [PubMed: 10637272]
62. Roato I, Grano M, Brunetti G, Colucci S, Mussa A, Bertetto O, Ferracini R. Mechanisms of spontaneous osteoclastogenesis in cancer with bone involvement. Federation of American Societies for Experimental Biology Journal 2005;19:228–230.
63. Theill LE, Boyle WJ, Penninger JM. RANK-L and RANK: T cells, bone loss, and mammalian evolution. Annual Review of Immunology 2002;20:795–823.
64. Cox M, Haddad JG. Lymphoma, hypercalcemia, and the sunshine vitamin. Annals of Internal Medicine 1994;121:709–712. [PubMed: 7944081]

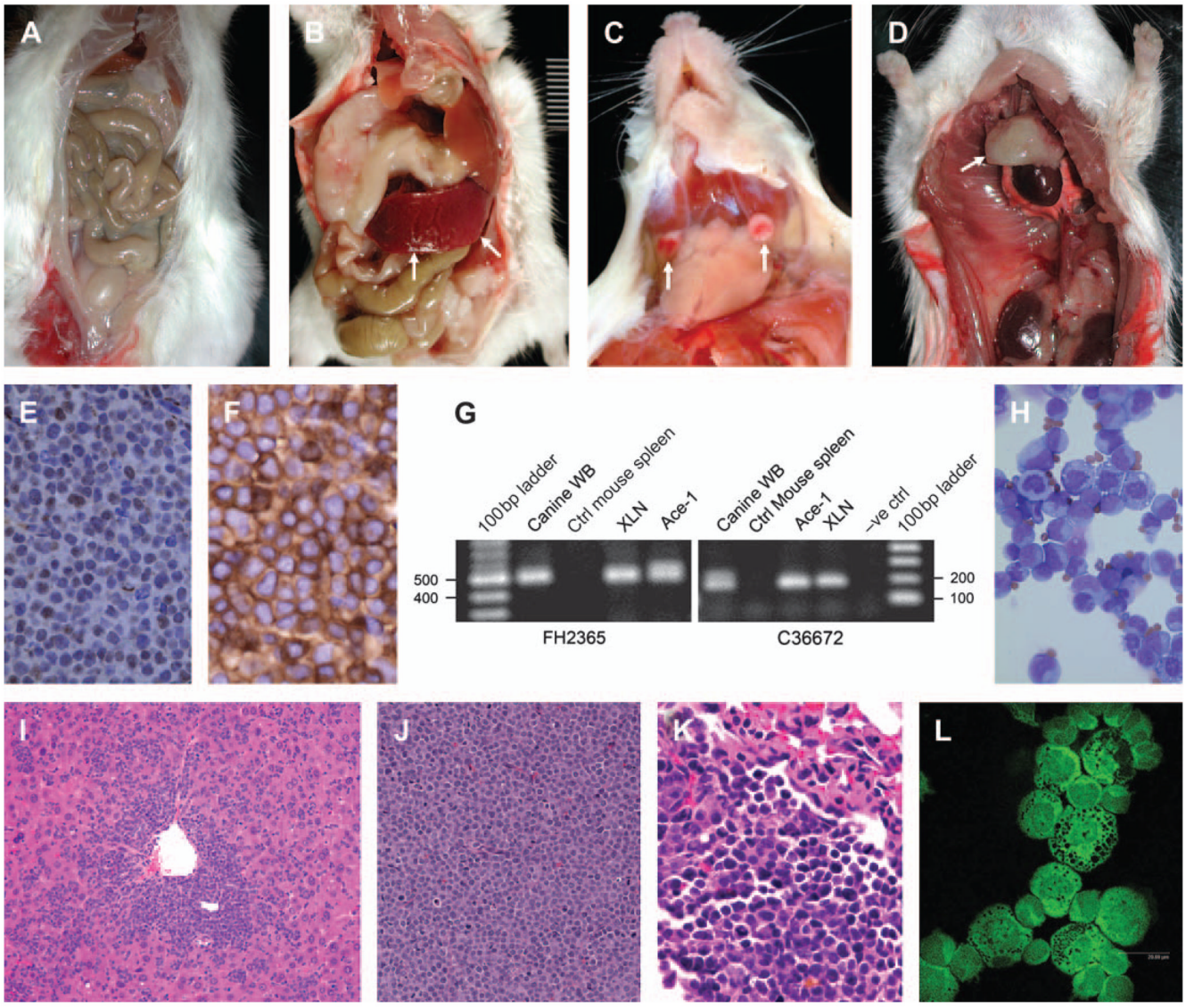

Figure 1.

Characterization of canine T-cell lymphoma xenografted in NOD/SCID mice. Photomicrographs of (A) control (ctrl) NOD/SCID mouse. NOD/SCID mouse with canine lymphoma xenograft (shown by arrows) in (B) the spleen, (C) the mandibular lymph nodes and (D) the thymus. (E) Negative immunohistochemistry for CD79 αcy (pan B-cell marker) in lymphoma of the mesenteric lymph node (immunoperoxidase; final magnification, 200×). (F) Positive immunohistochemistry for CD3 (pan T-cell marker) in lymphoma of the mesenteric lymph node (immunoperoxidase; final magnification, ×200). (G) PCR amplification of canine microsatellites. The specific products of 520 bp (FH2365) and 180 bp (C36672) were amplified from canine whole blood (WB), xenografted canine lymphoma, and a canine prostate cancer cell line (Ace-1) but not from control mouse spleen. (H) Lymphoma cells in the ascites fluid from the xenografted mouse (Wright ’ s stain; magnification, 200×). (I) Lymphoma in the liver of a NOD/SCID mouse (haematoxylin and eosin [H&E]; original magnification, 100×). (J) Diffuse lymphoma in the mesenteric lymph node of a NOD/SCID mouse (H&E; original magnification, 200×). (K) Lymphoma in the lungs of a NOD/SCID

mouse (H&E; original magnification, 200×). (L) PTHrP immunofluorescence in the cytoplasm and nucleus of lymphoma cells (fluorescein isothiocyanate; confocal imaging, 400×).

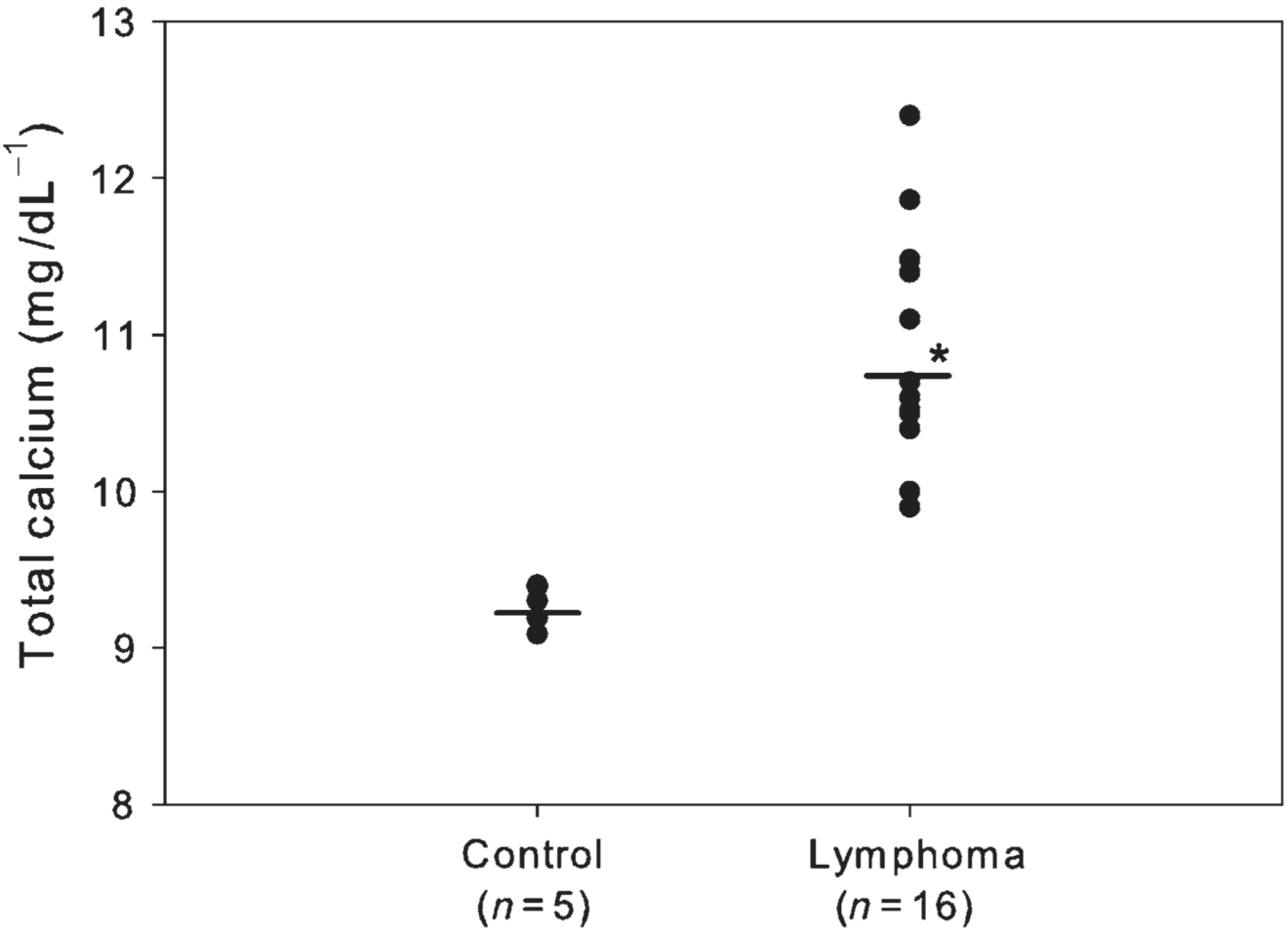

Figure 2.
Plasma total calcium concentrations (mg dL $^{-1}$). Mice engrafted with canine T-cell lymphoma had significantly (* $P < 0.05$) greater plasma total calcium levels (10.9 ± 0.8 mg dL $^{-1}$) than controls (9.2 ± 0.13 mg dL $^{-1}$). Bars indicate means.

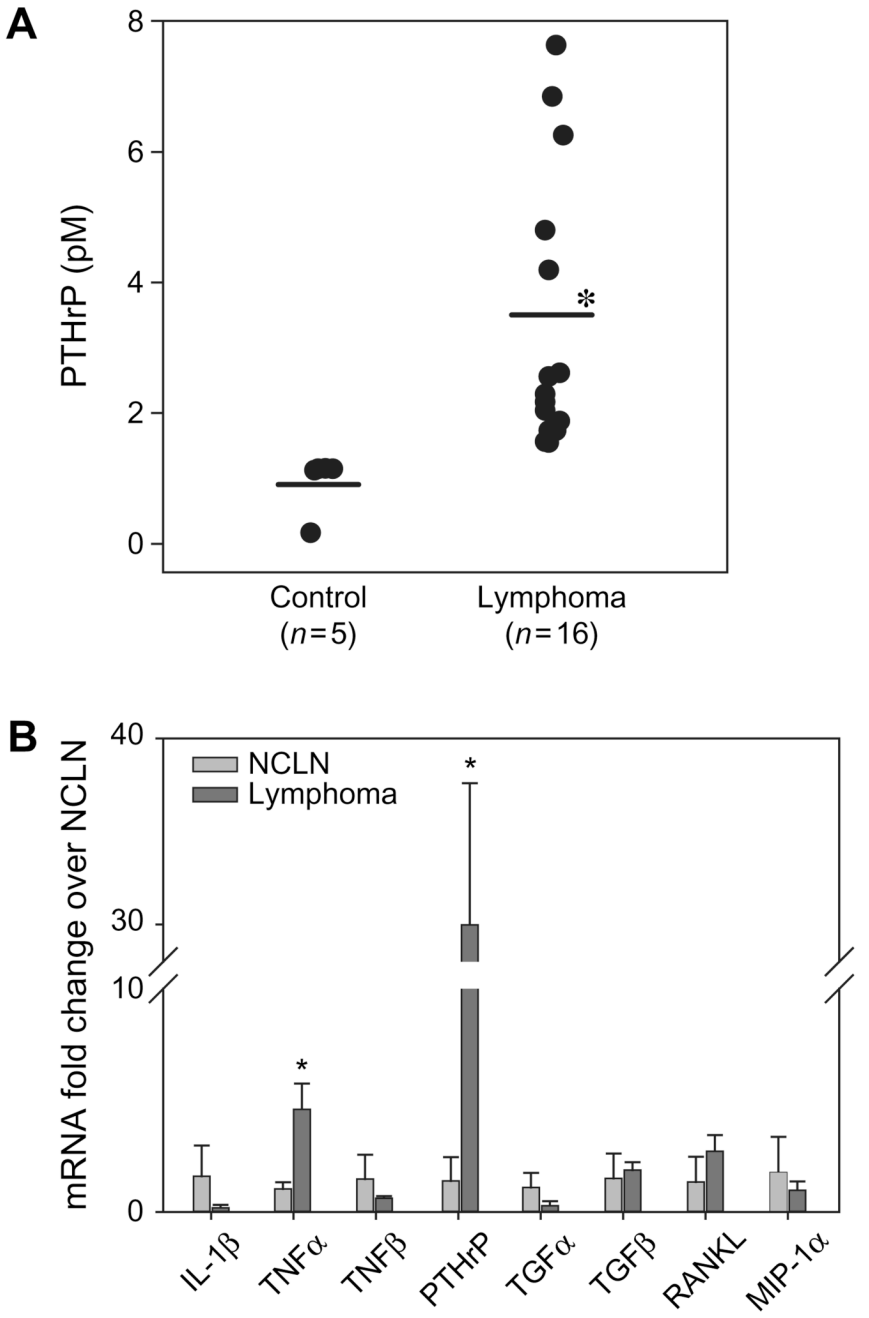

Figure 3.

Hypercalcaemic factors in the NOD/SCID mice xenografted with canine lymphoma. (A) Plasma PTHrP concentrations (pM). The xenografted NOD/SCID mice have increased concentrations of circulating PTHrP (3.2 ± 2.0 pM L^{-1}) ($P = 0.025$) compared to control mice (<1.5). Bars represent averages. (B) qRT-PCR for expression of mRNA for hypercalcaemic factors in the xenografted canine T-cell lymphoma. The mesenteric lymphomas expressed significantly higher levels of PTHrP and TNFα mRNA (* $P < 0.05$) than NCLN. No significant differences were observed in other cytokines examined. Bars represent the mean ± SD of three independent samples.

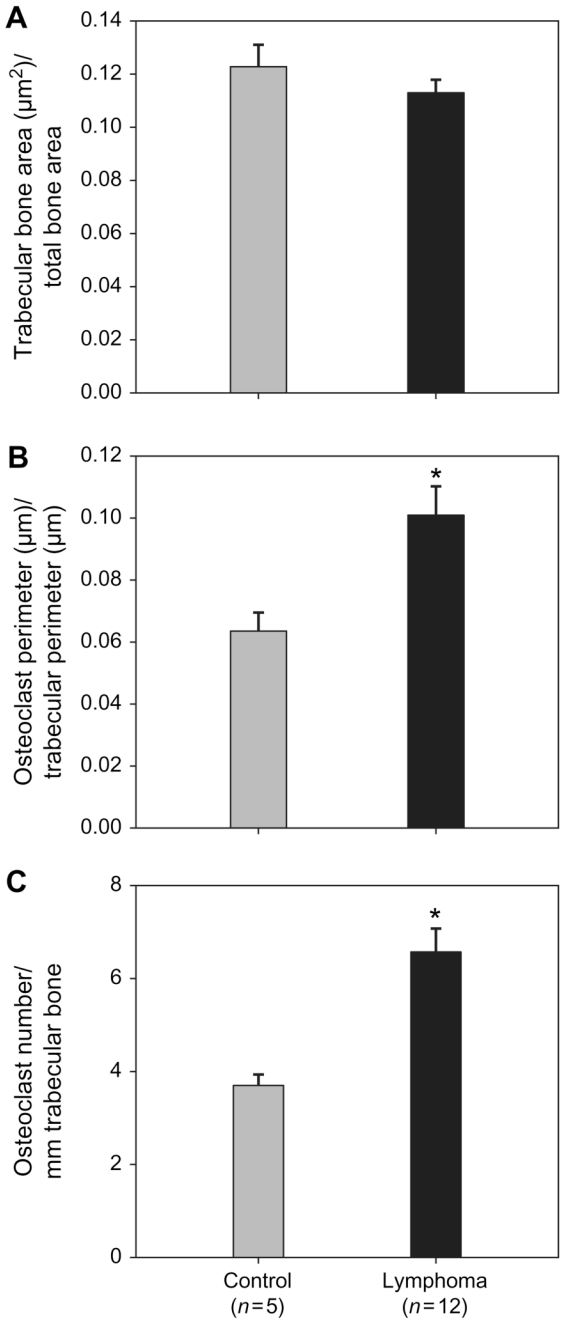

Figure 4.

Histomorphometry of tibiae of NOD/SCID mice xenografted with canine T-cell lymphoma. (A) There was no significant difference in the trabecular bone area between the control and the lymphoma-bearing NOD/SICD mice. (B) Per cent osteoclast perimeter was significantly increased (* $P < 0.005$) in the lymphoma-bearing mice compared with the controls. (C) Osteoclast number per millimetre of trabecular bone was significantly increased in lymphoma-bearing mice compared with controls, * $P < 0.05$. Bars represent the mean ± SE.

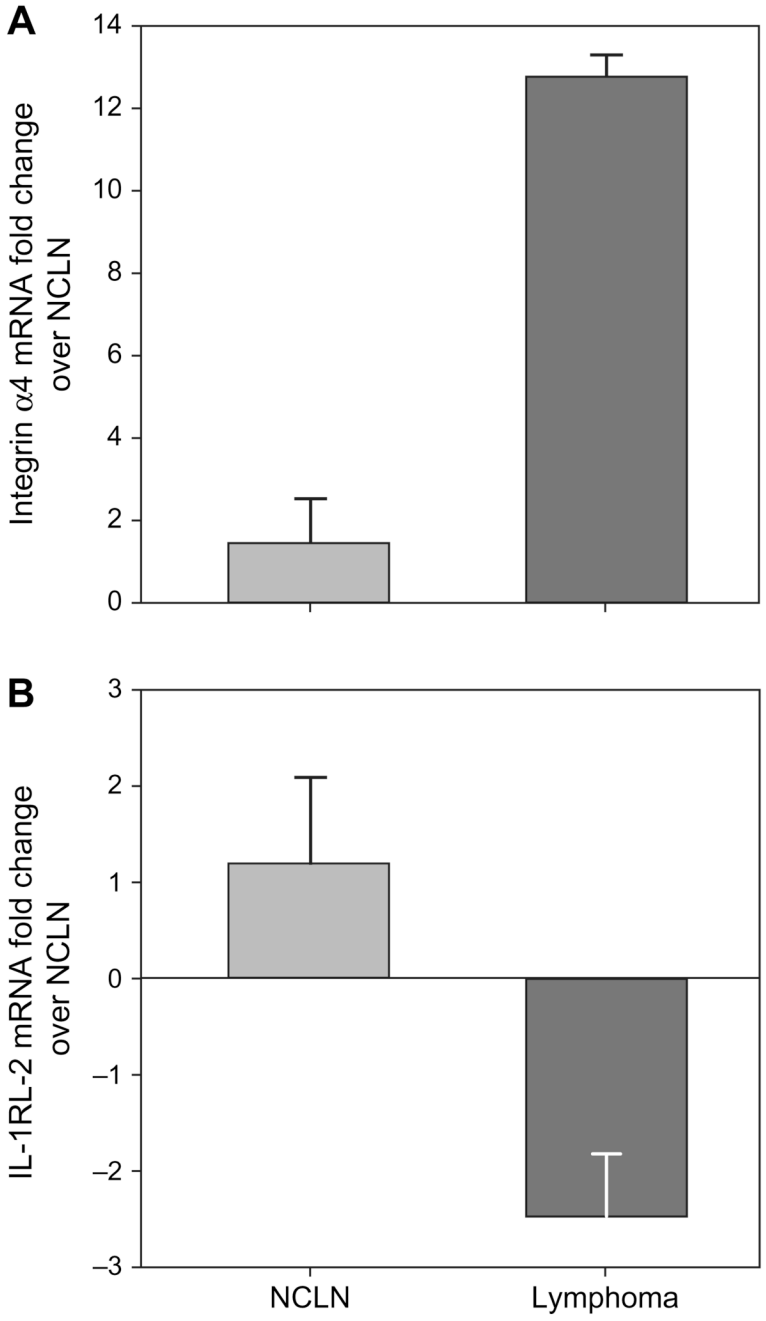

Figure 5.
qRT-PCR verification of microarray data. (A) Upregulation of integrin α4 mRNA in the primary tumour and the mesenteric lymphomas from the xenografted mice compared with the NCLN. (B) Downregulation of IL-1RL-2 mRNA in the primary tumour and the mesenteric lymphomas from the xenografted mice compared with NCLN.

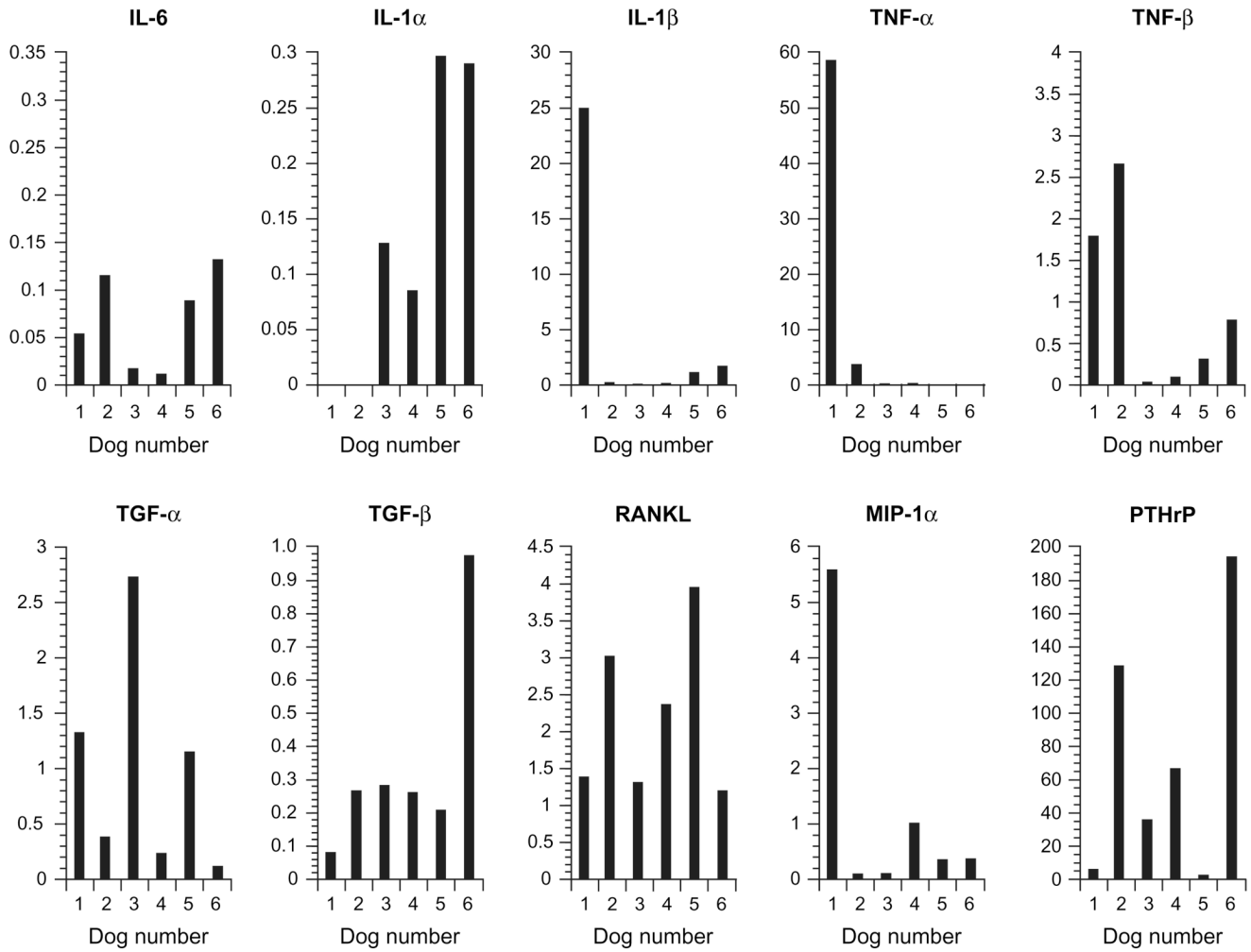

Figure 6.

Hypercalcaemic factors in canine T-cell lymphoma patients with hypercalcaemia. qRT-PCR analyses for mRNA expression for IL-6, IL-1α, IL-1β, TNFα, TNFβ, TGFα, TGFβ, RANKL, MIPα and PTHrP from dogs with T-cell lymphoma and hypercalcaemia normalized to NCLNs. Moderate to markedly elevated PTHrP and a mild upregulation of RANKL mRNA expression was present in most of the dogs with T-cell lymphoma and hypercalcaemia.

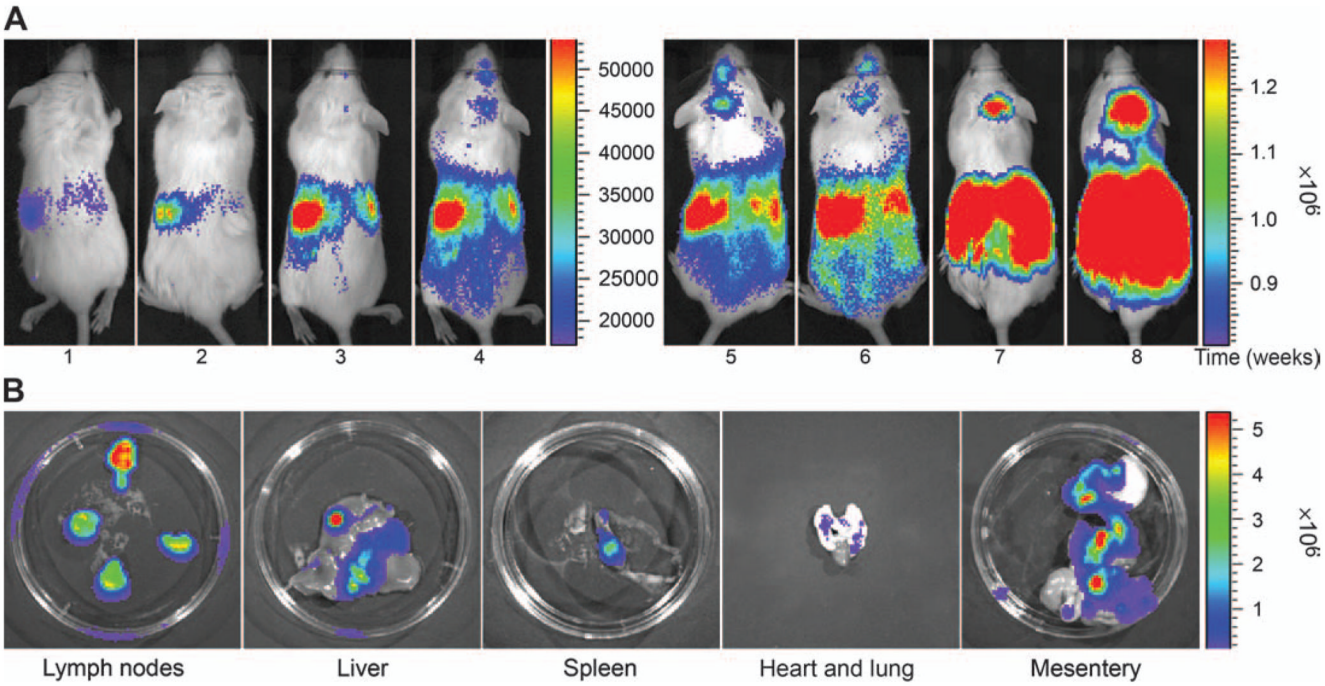

Figure 7.

BLI in mouse model of canine T-cell lymphoma. (A) Serial noninvasive BLI of canine T-cell lymphoma in NOD/SCID mice following intraperitoneal injection of luciferase/YFP-transduced lymphoma cells. Note the progressive increase in the photon intensities reflecting the progression of the lymphoma from weeks 1 to 8. The BLI signal intensity was measured as photons sec cm $^{-2}$. The colour bar to the right of the images represents the range of photon flux. (B) *Ex vivo* imaging of mesenteric lymphomas, liver, spleen, heart and lungs, and the gastrointestinal tract after euthanasia. Note the high photon intensities in the mesenteric lymphomas and along the mesentery.

Table 1

Primers used for qRT-PCR with accession numbers for each gene

Gene (accession number)	Forward primer	Reverse primer	Amplicon size (bp)
IL-1β (Z70047)	AGCTTTGGAGAAGCTGAAGAAGCC	TCCTGTAACTTGCAGTCCACCGAT	170
RANKL (NM_033012)	AGGTTGGGCCAAGATCTCCAACAT	TCAGCTGAAGATACTCTGTGGCGA	143
TGFα (NM_003236)	AGGTTTCTGGTGCAGGAGGACAA	AGCACACACGCGATGATGAGGA	160
TNFβ (M55913)	AGCACTTCATACAAGGCACCCTCA	ACCAGGAGGGAATTGTTGCTCAGA	141
MIP-1α (AF043339)	TAGTCGACTGCTTTGAGACCAGCA	CTTTCAGCTTCAGATCGGCCACAT	135
PTHrP (U15593)	AGCTCGGCCGCCGGCTCAA	GGAAGAATCGTCGCCGTAAG	93

Table 2

Histopathology in NOD/SCID mice xenografted with canine T-cell lymphoma

Organ	Number of mice with lymphoma/total number of mice
Mesentery	14/16
Spleen	14/16
Liver	12/16
Kidney	10/16
Lungs	8/16
Thymus	2/16

Table 3

List of genes differentially expressed in the xenografted canine T-cell lymphoma compared with NCLNs

Genes upregulated in lymphoma compared with NCLN	Fold increase
Adhesion molecules	
NCAM	6.1
Integrins	
Integrin α4	8.3
Integrin β7	10.2
Integrin α7	3.6
Integrin-αL	4.2
Cell surface proteins	
C3	8.3
CD3 gamma	4.4
CD3 epsilon	6.2
CD3 delta	5.8
CD3 zeta	3.1
Developmental factors	5.2
MFNG	3.8
SEMA4D	
G-protein-coupled receptors	
GPR 9-6	10.4
GPR10	4.8
Protease or related factor	
MMP-9	4.2
Signal transduction	
HDAC1	3.8
HDAC3	3.1
CBL	3.1
FAST-1	2.8
YWHAZ	4.8
CIS3	5.1
STAT 5A	3.6
ARHB/RhoB	4.2
PTPN5	2.8
TRIP	2.5
Cell cycle regulators	
Cyclin A2	3.6
CDK4	3.5
Apoptosis related	
TRADD	5.8
FADD	3.6
Eph family	

Genes upregulated in lymphoma compared with NCLN	**Fold increase**
EphB6	3.8
EphB4	4.2
TNF superfamily	
TNFRSF6B/DcR3	5.6
Binding protein	
LTBP4	3.1
Genes downregulated in lymphoma compared with NCLN	**Fold decrease**
TNF superfamily	
TNFRSF1B	20.2
EDAR	10.4
Adhesion molecules	
BCAM	4.4
Protease or related factor	
ADAM 12	6.2
Other factors	
NMA	10.2
Binding protein	
LBP	18.2
Interleukin receptors	
IL-1RL2	8.2
IL-18 RAP	4.8
Cell surface proteins	
RP105	4.8
SLAM	6.2
FGF family	
FGFR1	22.3
Neurotrophic group	
Ret	5.2
Chemokines	
MCP-1	2.6